SWITCHED $\mathcal{H}_\infty$ CONTROL STRATEGY OF AUTOMOTIVE ACTIVE SUSPENSIONS

A. Zin, * **O. Sename** * **and L. Dugard** *

* *Laboratoire d'Automatique de Grenoble, UMR CNRS-INPG-UJF, ENSIEG-BP 46, 38402 Saint Martin d'Hères Cedex, FRANCE.*
Email: {Olivier.Sename,Luc.Dugard}@inpg.fr

Abstract: The three main performance metrics in automotive suspensions are passenger comfort, suspension deflection, and road holding ability. It is well-known that these three objectives can not be reached at the same time. In order to reach them "individually", three linear $\mathcal{H}_\infty$ controllers are designed. At each moment, the desired performance requirement is chosen with a robust stable control strategy that switches between the three linear $\mathcal{H}_\infty$ controllers. The switched control logic is not developed in this study.

Keywords: Vehicle suspension, $\mathcal{H}_\infty$ control, Switched systems

1. INTRODUCTION

The suspension system is the main tool to achieve *ride comfort* and *road holding* for a vehicle. The design of a suspension is always based on a good compromise between these two targets, but structural limitations (like the *suspension deflection* limitation) prevent passive solutions from achieving the best performance for both goals (Hedrick, 1990). Originally, this trade-off was partially solved by the single optimal adjustment of a passive damper (Miller, 1988).

Hence, the development of computer-controlled suspension actuators has led to many control strategy designs based on various types of methodologies.

In robust synthesis, robust stability and performance can be guaranteed in the presence of plant uncertainties (see e.g. (Sammier *et al.*, 2003)), but these methods result in a controller which creates a trade-off between the different performance specifications, leading to some conservatism. An LPV method is proposed for a nonlinear model that guarantees the trade-off between passenger comfort and suspension deflection (Gaspar *et al.*, 2004), but this method is also conservative w.r.t. the design of LTI controllers that separately guarantee passenger comfort or suspension deflection. In (Altet *et al.*, 2003) the performance trade-off between ride comfort and road holding is considered as a hybrid system for a Crone suspension only.

In this paper, a control design for *active suspensions* of passenger vehicles is proposed. As shown in Fig. 1, this control strategy is developed and analyzed on a quarter-car system model $G(.)$, and the choice between a ride comfort/road holding/suspension deflection control strategy is guaranteed by a *robust switched* controller $K(s,\theta)$ [1], following the switching method presented in (Hespanha and Morse, 2002).

Here we consider the relative suspension deflection [2] has the available measure $y(t)$; $z(t)$ contains the signals to be controlled by the switching signal $\theta(t)$ and the control signal $u_{ca}(t)$. $z(t)$ are the sprung mass acceleration (for comfort control

[1] s is the Laplace variable

[2] Some technical definitions of an automotive suspension are given in section 2

objectif), the suspension deflection (in order to prevent the suspension travel limits), and the tire deflection (for road holding ability objectif). The exogenous signal $\theta(t)$ can be chosen according to the vehicle stability and the value of the suspension deflection. The disturbance signal $d(t)$ is the road profile that must be attenuated in order to obtained the request performances (ride comfort/road holding/suspension deflection).

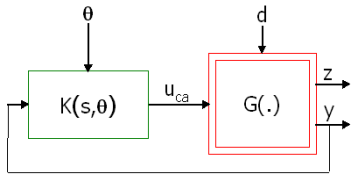

Fig. 1. Switched control configuration.

In automotive applications as suspension or engine control, controllers are often implemented using static maps. However the stability of the closed-loop system (subject to the controller changes) is not proved. Here the switching method will be proved stable in the active suspension control problem. The switched control logic (i.e. the choice of the trajectory of the signal $\theta(t)$) is not developed in this study.
This paper deals (section 2) with the quarter-car model of a suspension. In section 3, three linear $\mathcal{H}_\infty$ regulators are designed and a new state space realization is computed to guarantee the closed-loop system stability defined in Fig. 1. In section 4 some simulation results are presented to validate the approach.

2. THE QUARTER-CAR MODEL

The two quarter-car models representing a passive and an active suspension respectively, are shown in Fig. 2, where m_s is the sprung mass (quarter car body); m_{us} is the unsprung mass (wheel assembly); $F_{ks}(.)$ and $F_{kt}(.)$ are the vertical forces of the suspension and tire springs, respectively;

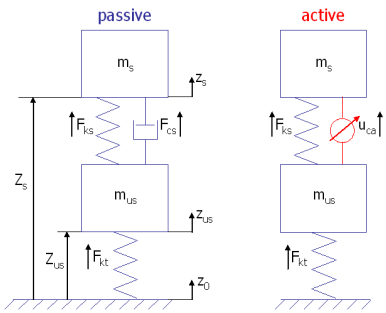

Fig. 2. Quarter-car suspension model.

$F_{cs}(.)$ and $u_{ca}(t)$ are the vertical forces of the passive and active suspension shock-absorbers, respectively; Z_s and Z_{us} are the absolute static displacements of the (loaded) suspension and tire springs; $z_s(t)$ and $z_{us}(t)$ are the relative vertical positions (around the steady-state displacements Z_s and Z_{us}) of the sprung and unsprung masses, respectively; $z_0(t) \equiv d(t)$ is the road profile. This model is usually used to analyze and/or to design suspension control laws; when the objective of the study is the dynamics of the vehicle, the suspension models are more complicated (see e.g. (Zin *et al.*, 2004)).
As mentioned in (Rossi and Lucente, 2004), the simplest controllers designed from a quarter car-model can be considered as better than those designed from more complicated models for their features of disturbance rejection, robustness and simplicity.
The dynamic of the nonlinear quarter-car model is given by the following set of differential equations (Kiencke and Nielsen, 2000):

$$\begin{cases} m_s\ \ddot{z}_s(t) &= -F_{cs}\Big(\dot{z}_s(t) - \dot{z}_{us}(t)\Big) + \\ & \quad - F_{ks}\Big(z_s(t) - z_{us}(t)\Big), \\ m_{us}\ \ddot{z}_{us}(t) &= F_{cs}\Big(\dot{z}_s(t) - \dot{z}_{us}(t)\Big) + \\ & \quad + F_{ks}\Big(z_s(t) - z_{us}(t)\Big) + \\ & \quad - F_{kt}\Big(z_{us}(t) - z_0(t)\Big),. \end{cases} \tag{1}$$

$F_{ks}(.)$ and $F_{cs}(.)$ are nonlinear functions shown in Fig. 3, while $F_{kt}(.)$ is approximated by a linear behavior, i.e. $F_{kt}(t) = k_t\ \Big(z_{us}(t) - z_0(t)\Big)$, where k_t is the vertical stiffness coefficient of the tire.

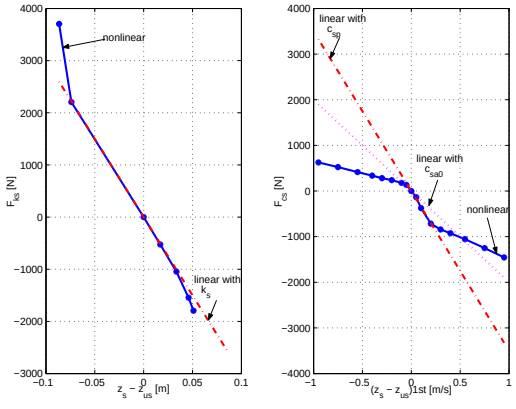

Fig. 3. Suspension force characteristics.

The model (1) can be written as :

$$\dot{x}(t) = f_p\Big(x(t)\Big) + B_1\ z_0(t), \tag{2}$$

where the state vector $x(t)$ may be chosen as:

$$x^T(t) = \Big[\dot{z}_s(t),\ z_s(t),\ \dot{z}_{us}(t),\ z_{us}(t)\Big].$$

With reference to Fig. 1 and 2 the following four models can be considered.

- The **nonlinear passive model** of reference described by (2) is used in section 4 for simulations in the time domain.

- The **nonlinear open-loop active suspension model**, called $G(.)$ in Fig.1, is obtained from equations (2) where $F_{cs}(.)$ is replaced by the active shock absorber force $u_{ca}(t)$. It is used in section 4 for simulations in the time domain.

- The **linear passive model** of reference obtained by a linear approximation of (2) is used in section 3 for simulations of the passive system in the frequency domain. From the linearized static maps $F_{sk}(.)$ and $F_{sc}(.)$, the coefficients of stiffness k_s of the spring and the coefficient of damping c_{sp} of the passive shock-absorber are found (see Fig. 3). This linear system can then be written as:

$$\dot{x}(t) = A_p\ x(t) + B_1\ z_0(t), \qquad (3)$$

where:

$$A_p = \begin{bmatrix} -c_{sp}/m_s & -k_s/m_s & c_{sp}/m_s & k_s/m_s \\ 1 & 0 & 0 & 0 \\ c_{sp}/m_{us} & k_s/m_{us} & -c_{sp}/m_{us} & -(k_s+k_t)/m_{us} \\ 0 & 0 & 1 & 0 \end{bmatrix},$$

$$B_1^T = \begin{bmatrix} 0 & 0 & k_t/m_{us} & 0 \end{bmatrix}.$$

- The **linear open-loop active model** used in section 3 for the designing of the linear $\mathcal{H}_\infty$ controllers, is the same as (3) where the coefficient of damping c_{sp} is replaced by $c_{sa}(t) = c_{sa0} + \Delta_{csa}(t)$; c_{sa0} is a positive coefficient and $\Delta_{csa}(t)$ is a signal that can be non positive (note that in the case of semi-active shock-absorber, the signal $c_{sa}(t)$ is always negative).
The active force is expressed by:

$$u_{ca}(t) = c_{sa}(t)\ \Big(\dot{z}_s(t) - \dot{z}_{us}(t)\Big).$$

and can be decomposed as:

$$u_{ca}(t) = c_{sa0}\ \Big(\dot{z}_s(t) - \dot{z}_{us}(t)\Big) + u(t), \qquad (4)$$

From (3) and (4), the new linear system can be written as:

$$\dot{x}(t) = A_a\ x(t) + B_1\ z_0(t) + B_2\ u(t), \qquad (5)$$

where

$$A_a = \begin{bmatrix} -c_{sa0}/m_s & -k_s/m_s & c_{sa0}/m_s & k_s/m_s \\ 1 & 0 & 0 & 0 \\ c_{sa0}/m_{us} & k_s/m_{us} & -c_{sa0}/m_{us} & -(k_s+k_t)/m_{us} \\ 0 & 0 & 1 & 0 \end{bmatrix},$$

$$B_2^T = \begin{bmatrix} 1/m_s & 0 & 1/m_{us} & 0 \end{bmatrix}.$$

As mentioned in section 1, in this study the suspension deflection is considered as the only available measure, which corresponds to:

$$y(t) = z_s(t) - z_{us}(t) = C_2\ x(t), \qquad (6)$$

where

$$C_2^T = \begin{bmatrix} 0 & 1 & 0 & -1 \end{bmatrix}.$$

The various parameters introduced in the previous equations represent the characteristics of a "medium" range passenger car with three persons on board and are given in table 1.

Table 1. Quarter-car model parameters.

$m_s(kg)$	$= 360$	$k_t(N/m)$	$= 208000$
$m_{us}(kg)$	$= 37.5$	$c_{sp}(N/m/s)$	$= 3500$
$k_s(N/m)$	$= 30000$	$c_{sa0}(N/m/s)$	$= 2000$

Remark 1. The control signal $u_{ca}(t)$ given by (4) requires also to know the deflection velocity $\dot{y}(t) = \Big(\dot{z}_s(t) - \dot{z}_{us}(t)\Big)$ which can be computed by cautious numerical derivation of the measure $y(t)$ (i.e. the suspension deflection) or directly measured by another sensor. The Fig. 4 shows an example of the control scheme that requires only the measure of the suspension deflection $y(t)$.

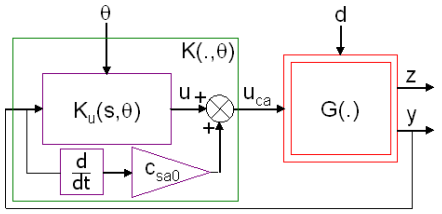

Fig. 4. Implementation of the control law.

3. SWITCHED $\mathcal{H}_\infty$ CONTROLLER DESIGN

In this section, the switched $\mathcal{H}_\infty$ controller $K_u(s,\theta)$ design procedure is presented.

Step 1. Design of LTI $\mathcal{H}_\infty$ controllers.
Three $\mathcal{H}_\infty$ controllers are designed for the quarter-car model (5)-(6),according to the objective to reach.
If the passenger comfort strategy is looked for, the first controller is designed to maintain the vertical acceleration of the sprung mass $\ddot{z}_s(t)$ as small as possible (at low/medium frequencies, see e.g. (Gillespie, 1992; Sammier *et al.*, 2003)). For a good road holding, the second controller acts to reduce the tire deflection $z_{deft}(t) = \Big(z_{us}(t) - z_0(t)\Big)$. Otherwise, the third controller is used to reduce the suspension deflection $z_{def}(t)$. In addition to these signals, the force $u_{ca}(t)$ provided by

the active shock-absorber must be controlled in order to prevent the saturation of the actuator. According to (5)-(6) the signal $z(t)$ to be controlled is selected as:

$$\begin{cases} z(t)^T = \Big[z_s(t),\ z_{deft}(t),\ z_{def}(t),\ u_{ca}(t)\Big], \\ z(t)^T = C_1\ x(t) + D_{11}\ z_0(t) + D_{12}\ u(t). \end{cases} \quad (7)$$

As in the usual $\mathcal{H}_\infty$ framework, the performance objectives are achieved via minimizing weighted transfer function norms. These functions define the performance specifications in the frequency domain.The considered scheme of the $\mathcal{H}_\infty$ control design interconnection is given in Fig. 5, where $n(t)$ is the sensor noise ($W_n(s)$ its weight); $W_d(s)$ is the weight used to scale the magnitude of the road disturbances; $W_z(s)$ is a diagonal matrix of the weighting functions applied to the controlled signal (7) which expresses the desired performances and robustness properties, i.e. $W_z(s) = diag\Big(W_{z0}(s), W_{cf}(s), W_{rh}(s), W_{df}(s), W_{uca}(s)\Big)$. The weighting functions for the three designs are given in table 2 and Fig. 6.

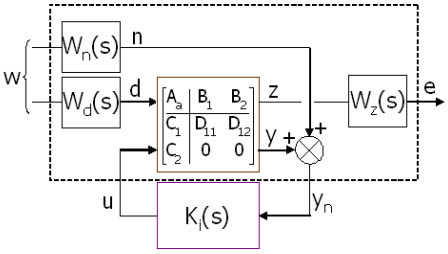

Fig. 5. $\mathcal{H}_\infty$ control design interconnection.

Remark 2 The design of the controller is made by taking in account the noise $n(t)$ for numerical aspects (see remark 1). In suspension control design, the measure of the suspension deflection is not noisy (Savaresi *et al.*, 2004).
Given γ, a prespecified attenuation level, a $\mathcal{H}_\infty$ suboptimal control problem is to design stabilizing controllers $K_i(s)$, $i = \{1, 2, 3\}$, that internally stabilizes the closed-loop system and minimizes the closed-loop transfer norm from the exogenous inputs $w(t)$ to the exogenous outputs $e(t)$: $\|e(t)/w(t)\|_\infty \leq \gamma$.
Here, the $\mathcal{H}_\infty$ suboptimal control problem is solved using Riccati equations (see e.g. (Zhou, 1998)).
Remark 3. Instead of controlling the vertical acceleration of the sprung mass $\ddot{z}_s(t)$ in (7), we have selected the vertical displacement of the sprung mass $z_s(t)$ which, as we will see, leads to good performances for $\ddot{z}_s(t)$.

Step 2. Controllers reduction order.
The controller design described in step 1 leads to three controllers of order 7 (for comfort design), 6 (for road holding design) and 6 (for deflection design). The controller for comfort design is reduced to the order 6 by the truncated balanced realization method (Skogestad and Postlethwaite, 1996) which is not necessary but suitable.

Table 2. Weighting functions selection.

i	Performance	W_{z0}	W_{cf}	W_{rh}	W_{df}	W_{uca}
1	Comfort	0.1	T_{cf}^{-1}	0	0	T_{cua}^{-1}
2	Road holding	0.1	0	T_{rh}^{-1}	0	T_{cua}^{-1}
3	Deflection	0.1	0	0	T_{df}^{-1}	T_{cua}^{-1}

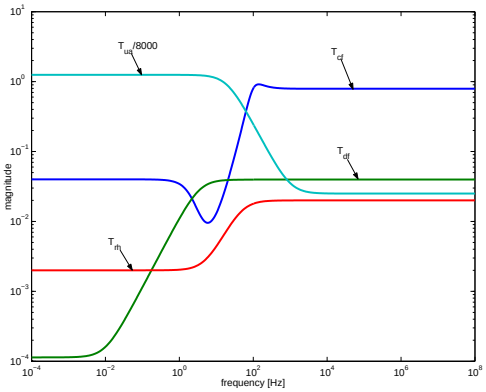

Fig. 6. Inverse of the weighting functions.

Step 3. Switching between controllers.
In this paragraph, realizations of the previous controllers are computed so that the switched closed loop system of Fig. 1 remains stable, no matter how we switch among the three controllers.
Let us first present a short background on stability of systems with impulse effects. For more details, see (Hespanha and Morse, 2002).
A switched system with state resetting at switching times, is called a system with impulse effect. Given the piecewise constant switching signal $\sigma(t)$, an homogenous system with impulse effect is described by:

$$\dot{\bar{x}}(t) = \bar{A}_i\ \bar{x}(t), \quad (8)$$

on intervals where the switching signal $\sigma(t)$ remains constant, and by

$$\bar{x}(t) = \bar{R}\Big(\sigma(t), \sigma(t^-)\Big)\ \bar{x}(t^-), \quad (9)$$

at each switching time t of $\sigma(.)$. The maps $\bar{R}\Big(\sigma(t), \sigma(t^-)\Big)$ are called reset matrices. Furthermore, the non-homogenous system associated to (8) is given by:

$$\dot{\bar{x}}(t) = \bar{A}_i\ \bar{x}(t) + \bar{B}_i\ \bar{w}, \quad (10)$$

on intervals where $\sigma(t)$ remains constant, and by (9) at each switching time t of $\sigma(.)$.
The following Lemma can be stated (Hespanha and Morse, 2002):
Lemma*Assume that there exist real symmetric matrices $\overline{Q}_i$, for which*

$$\bar{Q}_i \ \bar{A}_i + \bar{A}_i^T \ \overline{Q}_i < 0, \tag{11}$$

and

$$\bar{R}(i,j)^T \ \bar{Q}_i \ \bar{R}(i,j) \leq \bar{Q}_j, \quad i \neq j \tag{12}$$

hold. Then the homogeneous system (8)-(9) is exponentially stable. Moreover, for every switching signal $\sigma(t)$ and every bounded piecewise continuous signal $\bar{w}(t)$, the state $\bar{x}(t)$ of the non-homogenous system (10)-(9) is bounded.

The way to find new realizations of the three controllers designed in steps 1-2, for which (11)-(12) hold true for the switched closed loop of Fig. 1, is now detailed. The switching controller is realized as in Fig. 7 where the switched closed loop is represented. The signals $d_u(t)$ and $d_y(t)$ are two real bounded exogenous disturbances, one at the input and the other at the output of the system (5)-(6), respectively. On intervals where the switching signal $\theta(t)$ remains constant, the transfer functions $F_i(.)$ is given by:

$$\begin{cases} F_i(s) \ := K_i(s) \ \Big(1 - K_i(s) \ H_a(s)\Big)^{-1}, \\ H_a(s) \ = \ \{A_a, B_2, C_2, 0\}, \end{cases} \tag{13}$$

where $K_i(s)$ has been found in step 1-2 and $H_a(s)$ is the system (5)-(6).

At each switching time t of $\theta(t)$, the switched control is given by

$$x_c(t) = R_c\Big(\theta(t), \theta(t^-)\Big) \ x_c(t^-),$$

where $x_c(t)$ its the state vector of the controller.

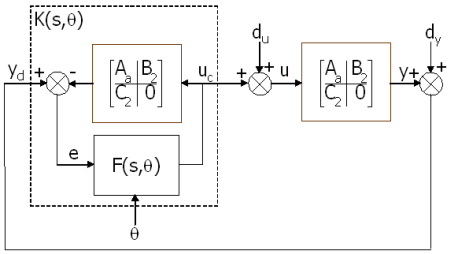

Fig. 7. Scheme of the stable realization of the switched controller.

As discussed in (Hespanha and Morse, 2002), if $H_a(s)$ is a stable system (which is true for (5)-(6)), the switched closed-loop system given in Fig. 7 is stable if and only if the system with impulse effect $F(s,\theta)$ is stable. Furthermore, there always exist stabilizable and detectable realizations $\{A_{fi}, B_{fi}, C_{fi}, D_{fi}\}$ [3] for each stable $F_i(s)$, such that

$$Q \ A_{fi} + A_{fi}^T \ Q < 0, \quad i = \{1,2,3\},$$

with $Q = I$. Therefore, from the previous lemma, one concludes that the new realization of $F(s,\theta)$ is stable in the particular case where $\bar{Q}_i = \bar{Q}_j = I$ and $\bar{R}(i,j) = I$ in (11) and (12), respectively. This corresponds to the multi-controller $K(s,\theta) = \{A_{ki}, B_{ki}, C_{ki}, D_{ki}, \theta\}$ in Fig. 1 with:

$$A_{ki} := \begin{bmatrix} A_a & B_2 \ C_{fi} \\ B_2 \ C_{fi} & A_{fi} \end{bmatrix}, \quad B_{ki} := \begin{bmatrix} B_2 \ D_{fi} \\ B_{fi} \end{bmatrix},$$

$$C_{ki} := \begin{bmatrix} D_{fi} \ C_2 \ C_{fi} \end{bmatrix}, \quad D_{ki} := D_{fi},$$

and $R_k(i,j) = I$.

4. SIMULATION RESULTS

A comparison between the closed-loop frequency responses of the linear active system and the linear passive model is shown in Fig. 8 for the suspension deflection and the acceleration of the sprung mass, and in Fig. 9 for the bounce of the sprung mass and the tire deflection.

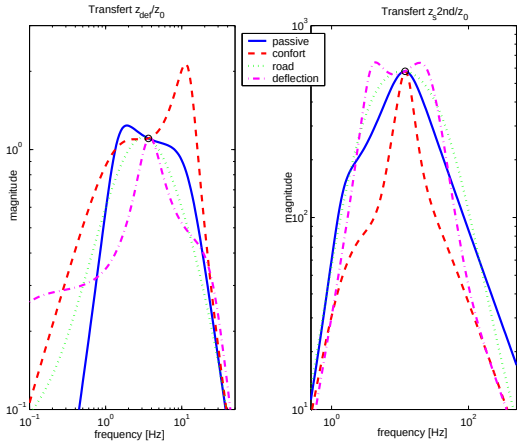

Fig. 8. Frequency domain results.

The dashed, dash-dot and dotted lines are the closed-loop frequency responses that result from comfort, road holding and suspension deflection designs, respectively; the solid lines are the passive linear model frequency response. The three main performance metrics are achieved individually.

Figures 10 and 11 show a comparison in the time domain between the closed-loop responses of the nonlinear active system and the nonlinear passive quarter-car model (1). The input is the road profile $z_0(t)$ is a series of steps of 6 cm of height; the switching signal $\theta(t)$ is constant from 0 to 6^- s (selected for comfort performances), and it changes at $t = 6$ s for road holding requirements. We can see that this leads to a different response for the controlled signal $z(t)$.

[3] see (Hespanha and Morse, 2002) for the computation

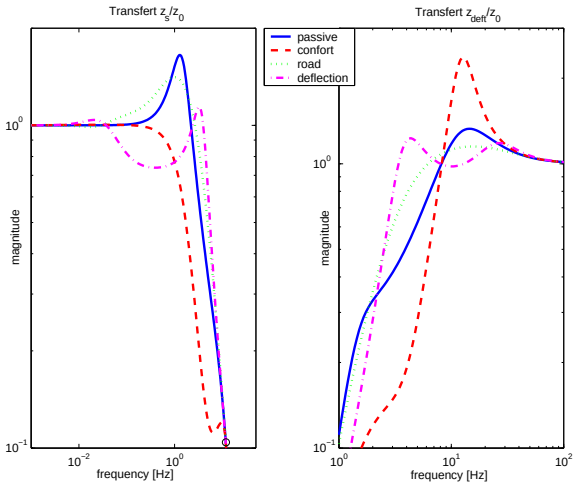

Fig. 9. Frequency domain results.

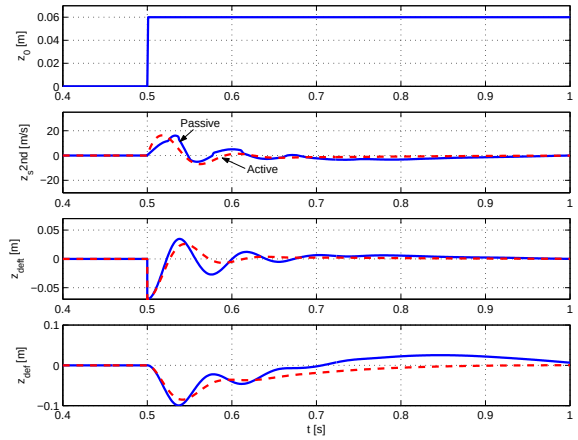

Fig. 10. Time domain results.

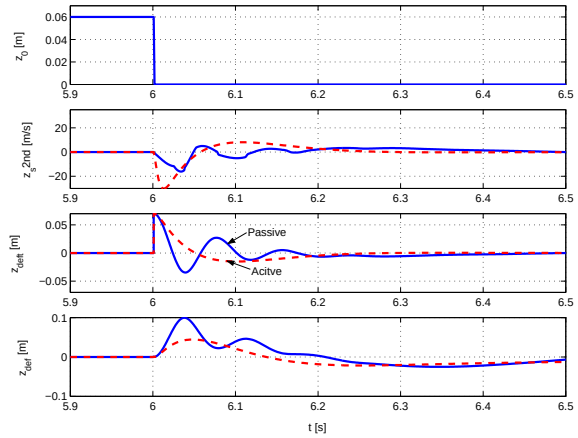

Fig. 11. Time domain results.

5. CONCLUSIONS AND FUTURE WORKS

In this paper a switched control method is used to achieve conflicting requirements of an automotive suspension. Simulations in the frequency and time domains show that good results in term of ride comfort, road holding and suspension deflection can be obtained while a single design could not reach the performance specifications.

This emphasizes the interest of this approach that ensures stability of the switching strategy.

An important issue for future research is the design of a switched *LPV* controller in order to take into account the nonlinearities of the characteristics of the suspension spring. Note that the theory developed in (Hespanha and Morse, 2002) can be extended for *LPV* stable plants.

REFERENCES

Altet, O., C. Nouillant, X. Moreau and A. Oustaloup (2003). La suspension *crone* hydractive : modelisation et stabilite. *Revue de l'electricite et de l'electronique* **9**, 84–93.

Gaspar, P., I. Szaszi and J. Bokor (2004). Active suspension using *lpv* control. *IFAC Symposium on Advances in Automotive Control, Salerno (Italy)* pp. 584–589.

Gillespie, T. D. (1992). *Fundamentals of Vehicle Dynamics*. Society of Automotive Engineers. USA.

Hedrick, J. K. (1990). Invariant properties of automotive suspensions. *Journal of Automotive Engineering* **204**(PartD), 21–27.

Hespanha, J. P. and A. S. Morse (2002). Switching between stabilizing controllers. *Automatica* **38**(11), 1905–1917.

Kiencke, U. and L. Nielsen (2000). *Automotive Control Systems For Engine, Driveline, and Vehicle*. Society of Automotive Engineers. Berlin Heidelberg.

Miller, L. R. (1988). Tuning passive, semi-active, and fully active suspension system. *IEEE 27th Conference on Decision and Control* pp. 2047–2053.

Rossi, C. and G. Lucente (2004). $\mathcal{H}_\infty$ control of automotive semi-active suspensions. *IFAC Symposium on Advances in Automotive Control, Salerno (Italy)* pp. 578–583.

Sammier, D., O. Sename and L. Dugard (2003). Skyhook and $\mathcal{H}_\infty$ control of semi-active suspensions: Some practical aspects. *Vehicle System Dynamics* **39**(4), 279–308.

Savaresi, S. M., E. Siliani and S. Bittanti (2004). Semi-active suspensions: an optimal control strategy for a quarter-car model. *IFAC Symposium on Advances in Automotive Control, Salerno (Italy)* pp. 572–577.

Skogestad, S. and I. Postlethwaite (1996). *Multivariable Feedback Control*. Wiley. New York.

Zhou, K. (1998). *Robust Optimal Control*. Prentice-Hall. New York.

Zin, A., O. Sename and L. Dugard (2004). A nonlinear vehicle bicycle model for suspension and handling control studies. *IFAC International Conference on Advances in Vehicle Control and Safety, Genoa (Italy)*. october 2004.